

A simple approach for measuring FRET in fluorescent biosensors using two-photon microscopy

Richard N Day¹, Wen Tao² & Kenneth W Dunn²

¹Department of Cellular and Integrative Physiology, Indiana University School of Medicine, Indianapolis, Indiana USA. ²Department of Medicine, Division of Nephrology, Indiana University Medical Center, Indianapolis, Indiana, USA. Correspondence should be addressed to R.N.D. (rnday@iupui.edu).

Published online 29 September 2016; doi:10.1038/nprot.2016.121

Genetically encoded fluorescent protein (FP)-based biosensor probes are useful tools for monitoring cellular events in living cells and tissues. Because these probes were developed for one-photon excitation approaches, their broad two-photon excitation (2PE) and poorly understood photobleaching characteristics have made their implementation in studies using two-photon laser-scanning microscopy (TPLSM) challenging. Here we describe a protocol that simplifies the use of Förster resonance energy transfer (FRET)-based biosensors in TPLSM. First, the TPLSM system is evaluated and optimized using FRET standards expressed in living cells, which enables the determination of spectral bleed-through (SBT) and the confirmation of FRET measurements from the known standards. Next, we describe how to apply the approach experimentally using a modified version of the A kinase activity reporter (AKAR) protein kinase A (PKA) biosensor as an example—first in cells in culture and then in hepatocytes in the liver of living mice. The microscopic imaging can be accomplished in a day in laboratories that routinely use TPLSM.

INTRODUCTION

The use of TPLSM imaging to monitor the signals from biosensor proteins in living animals is of interest to many laboratories because it allows noninvasive detection of spatial and temporal characteristics of specific cell signaling or metabolic events. These genetically encoded biosensor proteins contain reporter modules that typically consist of FPs that are directly linked to sensing units that detect specific cellular events¹. Many biosensor probes rely on FRET to report the changes in protein conformation that occur in response to the cellular event^{1–6}. There are, however, substantial challenges to the use of TPLSM to detect the FRET signals from biosensor probes in intact tissues; these issues fall into three general categories: (i) issues related to the 2PE characteristics of the biosensor probes; (ii) difficulties in expressing the genetically encoded biosensors in the desired cell type in living animals; and (iii) problems associated with conducting high-resolution microscopy in living animals. These three challenges are discussed further in the following sections, but this Protocol specifically addresses the first issue: identification, characterization and validation of a FRET-based FP biosensor suitable for TPLSM in intact tissues.

Optimized probes for TPLSM

Many existing biosensor probes that were developed for one-photon excitation may perform poorly (or not at all) under 2PE. Even those probes that perform well under 2PE may not be efficiently excited by the narrow range of wavelengths accessible with the titanium sapphire (Ti-sapphire) lasers used in most TPLSM systems (tunable from 690 to 1,040 nm, but peaking between 750 and 850 nm). Many biosensor assays are based on ratiometric measurements of images collected using two different excitation wavelengths. This complicates measurements by TPLSM because most FPs have broad two-photon cross-sections, limiting the ability to selectively excite one or the other FP. Furthermore, most TPLSM systems are equipped with a single IR laser, and thus the collection of ratiometric FRET measurements may require retuning of the laser between image acquisitions—a process that is slow (precluding dynamic studies) and introduces measurement errors because of changes in laser alignment. Finally, photobleaching processes

that occur under 2PE are poorly understood. Unlike that of single-photon excitation, the rate of photobleaching under 2PE increases exponentially with illumination power, sometimes increasing to the third or fourth power of the illumination level^{7,8}. As differences in the susceptibility of the donor and acceptor FPs to photobleaching can affect ratiometric measurements, it is particularly important to use FPs that are photostable and free from photoswitching behavior.

In vivo expression of FP biosensors

The sequences that encode the biosensor probes are easily incorporated into plasmid or viral vectors that allow their transfer into living cells or organisms. The use of suitable cell type-specific promoters can restrict the expression of the biosensors to specific tissues, and the probes can be directed to specific subcellular organelles by incorporating suitable targeting sequences. The fluorescence signals from biosensor probes have been successfully imaged in a wide variety of organisms. For example, transgenic *Caenorhabditis elegans*, *Drosophila* and zebrafish have been generated that express calcium-sensing biosensor proteins^{9–11}. In general, the imaging of biosensor activities in transgenic mice, however, has been proven to be more difficult¹². A problem often encountered with transgenes that have been stably integrated into mice is low-level expression resulting from transgene silencing or recombination events that occur between the highly homologous sequences encoding the sensor FPs^{13,14}. Transgenic mice generated by transposon-mediated gene transfer methods have been reported to have higher levels of biosensor expression^{13–15}. Transgenic biosensor mice that express a variety of different probes, including sensors for chloride¹⁶, calcium^{17,18} and voltage¹⁹, are available commercially (The Jackson Laboratory) and might be useful for specific intravital imaging applications. Transgenic mice expressing fluorescent biosensors for PKA, Erk, Rac and Ras are also available from Japan's National Institutes of Biomedical Innovation, Health and Nutrition. Further, there are published studies reporting transgenic biosensor mice with ubiquitous tissue distribution^{13,19} or restricted tissue expression¹². The critical question for investigators is whether the biosensor expression is sufficiently high in the

desired tissue in a particular mouse model to obtain unambiguous measurements of changing cell signaling events¹².

Viral transduction is an alternative approach that offers rapid biosensor probe expression in living animals without the need for lengthy breeding strategies to achieve stable expression. However, the challenge for *in vivo* administration of viral vectors is to obtain expression of the biosensor probes in the relevant cell types. The expression of probes in a particular tissue can be achieved using cell type-specific promoters that restrict the biosensor expression to the target cells. However, if the cells of interest can be identified based on morphology, it might not be necessary to achieve selective expression in specific cell populations. Further, the systemic administration of unmodified adenovirus (Ad) generally results in the accumulation of the transgene in the liver and spleen²⁰, and thus the tropism to these organs can be exploited for imaging studies.

High-resolution microscopy in living animals

Intact, living organisms present unique challenges for microscopy. First, the physiological welfare of the animal must be continuously monitored and maintained while the animal is on the microscope stage. Second, in most cases, the tissue of interest must be surgically exposed, requiring the development of methods for anesthesia and delicate surgery. Third, the tissue must be immobilized so that motion induced by respiration and the heart-beat is reduced to submicron levels.

The solutions to these challenges vary depending on the equipment used and the particular organ to be imaged. In our studies of kidney and liver^{21–24}, an inverted microscope stand is used to image the surgically exposed organs that are secured to a glass-bottom dish (Fig. 1). The anesthetized animal is placed on the microscope stage, and the animal's temperature is maintained using a heating pad and monitored using a rectal thermometer. Generally, tissue motion can be minimized by careful placement of the tissue, and can be reduced further by bonding small regions of the tissue to the coverglass with cyanoacrylate adhesive. In addition, gating the image collection to respiration can minimize the motion artifacts in tissues such as the lung^{25,26}. Finally, motion-induced distortions can be eliminated from the collected images using various methods of digital image analysis^{27–31}.

Quantitative intravital microscopy is also complicated by the inevitable loss of signal that occurs when imaging highly scattering biological tissues. Therefore, the intensity measurements obtained from different depths cannot be directly compared. In this regard, using FRET-based biosensors can be advantageous. The ratio images obtained from biosensors will be minimally affected by depth, provided that the scattering and absorption do not vary substantially for the emission wavelengths of the probe. Although we find no evidence of an effect of depth on FRET measurements obtained *in vivo*, minor effects were observed in other studies³². Therefore, biosensor measurements collected over a large range of depths should be evaluated for systematic effects of depth on the FRET ratio. In general, the effects of depth on ratiometric measures can be minimized by using non-descanned detectors that are less susceptible to the effects of light scatter, and by avoiding FPs with widely different emission spectra.

Development of the protocol

Previously, we described the characterization of FPs for FRET biosensor probes specifically intended for intravital imaging using

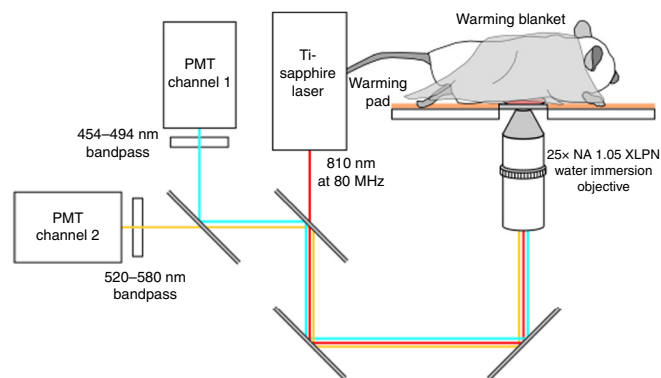


Figure 1 | Schematic overview of the setup for measuring biosensor activity in a living animal. After viral transduction of a biosensor probe in mice, activity of the probe is monitored in the anesthetized animal. The procedure uses selective 2PE of mTurquoise at 810 nm to make ratiometric FRET measurements *in vivo*. To image probe activity in the liver, the left lateral lobe of the liver is carefully lifted and secured to a glass-bottom plate. The mouse is then placed ventral side down on a heated microscope stage and covered with a warming blanket, and the liver is imaged using a long-working-distance water-immersion objective. PMT, photomultiplier tube.

TPLSM³³. As the cyan FPs (CFPs) are optimally excited at close to the power maximum of the Ti-sapphire lasers used in most TPLSM systems, we focused our evaluations of potential FRET donors on the newer variants of the CFPs that have improved brightness and photostability, and no photoswitching behavior^{34–37}. On the basis of previous studies demonstrating that wavelengths near 800 nm can be used for relatively selective excitation of CFP over yellow FP (YFP)^{38,39}, we focused our evaluations of potential FRET acceptors on newer, improved variants of YFP. On the basis of these studies, we identified monomeric (m)Turquoise³⁵ and mVenus⁴⁰ as optimal FPs for TPLSM. We found that illumination at 810 nm efficiently excited mTurquoise with minimal direct excitation of mVenus³³. The selective excitation of mTurquoise at 810 nm allows ratiometric FRET measurements *in vivo* using TPLSM at a single excitation wavelength. Moreover, the use of the CFP and YFP is compatible with most TPLSM configurations.

A critical step in the acquisition of measurements from FRET-based biosensors is validation of the sensitivity of the method. It is necessary to demonstrate that measurements of subtle changes in the FRET ratio truly reflect the responses of the biosensor to cellular events. In general, FRET measurements should be reproduced using multiple methods. For example, FRET estimates based on measurements of sensitized emissions should be complemented with estimates from acceptor photobleaching or fluorescence lifetime measurements³³. Given the inherent challenges of intravital microscopy, our goal was to develop a protocol that would minimize the validation studies that must be conducted. We accomplish this by providing a set of completely validated FRET standards and a simple method by which end users can characterize and optimize FRET measurements in their own systems.

Overview of the procedure

Here we describe a protocol in which a TPLSM system can be optimized and validated for FRET measurements in studies of cultured cells, before studies in living animals (Fig. 2). We demonstrate intravital FRET biosensor imaging using an AKAR biosensor of PKA activity, expressed by adenoviral transduction of the mouse liver.

PROTOCOL

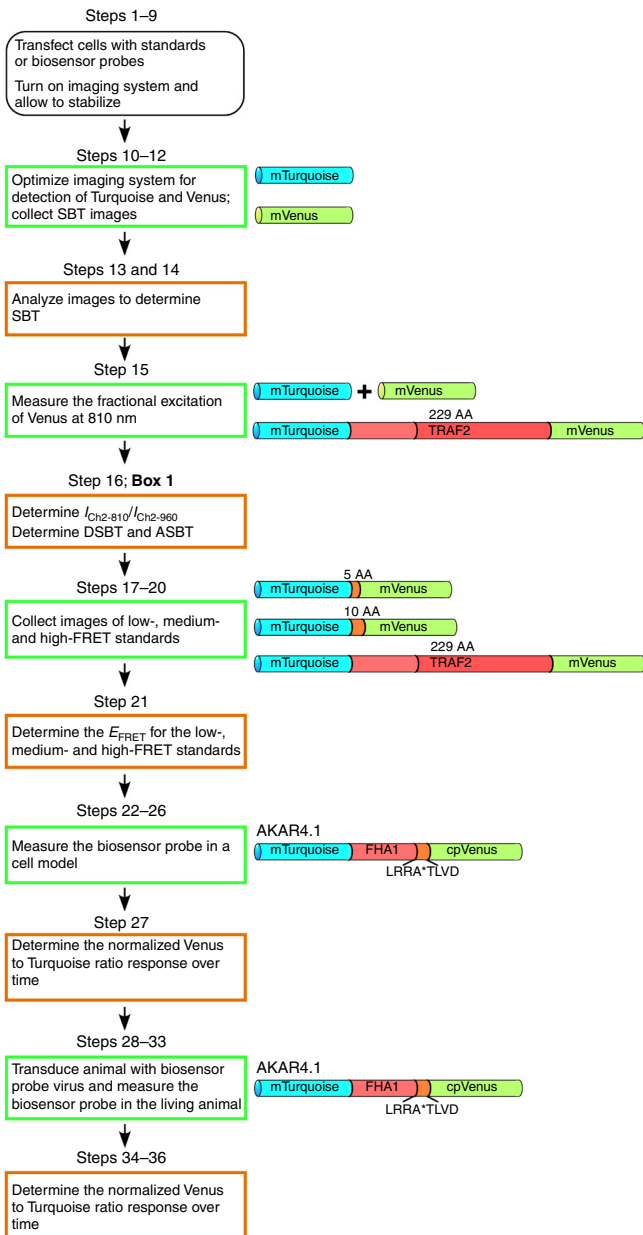


Figure 2 | Schematic workflow of the procedure and constructs described in **Table 1**. The procedure starts with transfection of cells (PROCEDURE Steps 1–8) with a series of standards that are used to evaluate and optimize the TPLSM system, and to determine the SBT components when using 2PE at 810 nm (PROCEDURE Steps 9–16). Then, the FRET standards are used to evaluate the sensitivity of the system for the accurate measurement of E_{FRET} (PROCEDURE Steps 17–21). The biosensor probe of interest is then verified in a cell model by measuring changes in the Venus to Turquoise ratio over time in response to suitable activators of the targeted signaling pathway (PROCEDURE Steps 22–27). Once the system and biosensor have been verified, studies in the living animal are conducted (PROCEDURE Steps 28–36).

Our approach to intravital measurements of FRET biosensor activity involves four stages: (i) characterization of the emission spectra and the determination of spectral cross-talk correction factors for the donor and emission FPs in the user's system; (ii) validation of the experimental system for measuring FRET using FRET standards expressed in cells in culture; (iii) validation of the FRET

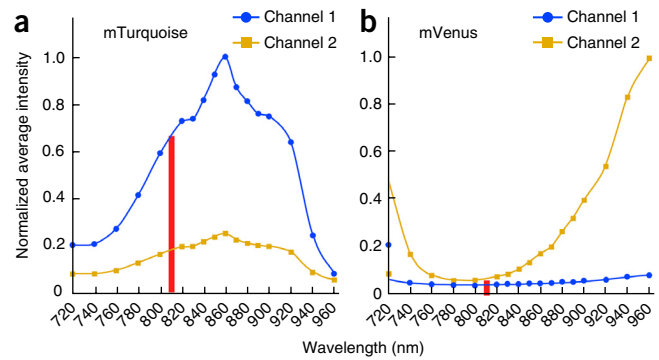


Figure 3 | 2PE spectral scan of the indicated FPs expressed individually in living HEK-293 cells. **(a,b)** The relative 2PE spectral scans for **(a)** mTurquoise and **(b)** mVenus were acquired from living cells by measuring fluorescence emissions over a range of excitation wavelengths at a constant laser power and a detector scaling factor of 1; the red bar indicates excitation at 810 nm, used in this protocol. To provide fluorescence excitation spectra that were independent of variations at the output of the laser at different wavelengths, spectral variation in laser power was eliminated by adjusting the laser power to a constant value at each wavelength, as measured using a Thorlabs PM100D power meter with λ correction, mounted on the microscope stage³³. The emission signals at the different excitation wavelengths were simultaneously detected in channel 1 (cyan, 454–494 nm) and channel 2 (yellow, 520–580 nm), and the images were acquired at each wavelength step, as described in the Experimental Design section. Image adapted with permission from ref. 33), American Physiological Society.

biosensor for measurements from cells in culture; and (iv) measurement of FRET biosensor responses in cells in living animals.

Measurement of spectral cross-talk correction factors. The imaging protocol described here exploits the relatively selective 2PE of mTurquoise³⁵ over mVenus⁴⁰ using illumination at 810 nm, which enables the measurement of FRET ratios from single, two-channel images (**Fig. 3**). However, the accurate measurement of FRET efficiencies (E_{FRET}) requires the application of correction factors for spectral cross talk (**Box 1**). These correction factors are entirely dependent on the configuration and performance of the microscope system, and must be measured for each system.

Characterization and validation of FRET measurements using FRET standards. The FRET standards are critical tools for both verifying the biological model and optimizing the particular imaging system used for FRET measurements⁴¹. By providing a range of calibrated, reproducible E_{FRET} values, the FRET standards allow the user to evaluate the performance of the system for the detection of FRET, and, importantly, allow an assessment of the sensitivity of the measurements (described in **ANTICIPATED RESULTS**). We have developed plasmids for a set of fully validated FRET standards, based on mTurquoise and mVenus (see **Fig. 2**; sequence information is provided in the **Supplementary Data** plasmids are available from the authors upon request). Measurements of E_{FRET} obtained from living cells expressing these standards (using the approach described in **Box 1**) are used to validate and optimize the user's system for the detection of FRET in mTurquoise–mVenus-based biosensors.

Validation of FRET biosensor probe activity in cultured cells. To verify and fully characterize the performance of the FRET biosensor in the user's system, preliminary studies are conducted in cultured cells; these can be manipulated to identify the full range

Box 1 | Digital analysis of SBT for the determination of FRET efficiency ● TIMING ~ 1 h

The optical pathway of the microscope system must be optimized for the detection of the mTurquoise–mVenus-based biosensor probe when excited at 810 nm. This is achieved by imaging cells that express either mTurquoise or mVenus alone (PROCEDURE Steps 12–14). Spectral scanning on systems with spectral detectors, or careful selection of emission filters on filter-based systems, will allow the user to adjust the optimal bandwidth for detection of the donor and acceptor signals (PROCEDURE Step 11). Once the donor and acceptor emission bandwidths are set, it is then necessary to measure the contributions of SBT to the signals detected in the FRET channel (excitation 810 nm, acceptor emission). The subtraction of the SBT signals from the signal that is detected in the FRET channel (FRET_{raw}) provides the corrected FRET (FRET_{corr}) signal⁵¹:

$$\text{FRET}_{\text{corr}} = I_{\text{FRET}} - A \cdot I_{\text{FRET}} - B \cdot I_{\text{Turq}} \tag{1}$$

Correction for acceptor SBT (ASBT). The ASBT signal arises from the direct excitation of mVenus at 810 nm. Correction factor A (equation 1) is used to remove ASBT. Measurements from cells expressing only mVenus are obtained using both 810-nm and 960-nm excitation to determine the fraction of the acceptor signal that arises from the direct excitation of mVenus at 810 nm. For our system, we determined that the ASBT fraction was 0.030. Because this protocol uses a single excitation wavelength (810 nm) to measure FRET standard and biosensor activity, it is also necessary to approximate the intensity in the acceptor channel (Ch2-960) from the measurement at 810 nm (i.e., the fractional excitation of mVenus at 810 nm). This is accomplished by measuring the average $I_{\text{Ch2-810}}/I_{\text{Ch2-960}}$ ratio from cells expressing a mixture of mTurquoise and mVenus, and cells expressing the low-FRET standard (Turquoise-TRAF-Venus). For our system, the average ratio was 0.344. Therefore, multiplication of the acceptor intensity measured with excitation at 810 nm by 2.91 (1/0.344) provides an approximation of the intensity in the acceptor channel, to allow correction for ASBT. For our microscope system, correction factor A is $2.91 \times 0.03 = 0.087$.

Correction for donor SBT (DSBT). Correction factor B (equation 1) is used to remove DSBT, the signal detected in the acceptor channel that results from donor emission bleed-through, and is determined from cells expressing only mTurquoise. Measurements from the donor-alone cells excited at 810 nm allowed us to determine that the donor bleed-through fraction was 0.295 on our system. Thus, the FRET_{corr} can be determined as follows:

$$\text{2PE FRET}_{\text{corr}} = I_{\text{FRET}} - 0.087 \cdot I_{\text{FRET}} - 0.295 \cdot I_{\text{Turq}} \tag{2}$$

Determining FRET efficiency (E_{FRET}) for the FRET standards. The validation of the imaging system is accomplished by measurement of the FRET standards. Here, measurements are acquired from cells expressing a low E_{FRET} standard (mTurquoise-TRAF-mVenus), and two high E_{FRET} standards (mTurquoise-5AA-Venus and mTurquoise-10AA-Venus), as described in ANTICIPATED RESULTS. The low E_{FRET} standard provides an indication of the threshold of detection, whereas the measurements from the two different high E_{FRET} standards allow the user to assess the sensitivity of the system.

The E_{FRET} value is calculated as previously described^{33,51,52} using the following equation:

$$E = D_{\text{lost}}/D_{\text{total}} = D_{\text{lost}}/(D_{\text{lost}} + D_{\text{remains}}) \tag{3}$$

where

$$D_{\text{lost}} = \text{FRET}_{\text{corr}} \cdot (QY_{\text{d}}/QY_{\text{a}}) \cdot (S_{\text{d}}/S_{\text{a}}) \cdot (G_{\text{d}}/G_{\text{a}}) \tag{4}$$

and

$$D_{\text{remains}} = I_{\text{Turq-810}} \tag{5}$$

QY_{d} and QY_{a} denote the quantum yields of the donor and acceptor, respectively, where the quantum yield ratio for mTurquoise and mVenus is 1.474 (refs. 35,40). S_{d} and S_{a} denote the spectral sensitivities of the donor and acceptor channels, respectively. The $S_{\text{d}}/S_{\text{a}}$ ratio is approximated by the bandwidth ratio of channel 1 and channel 2. G_{d} and G_{a} are the detector gains for the donor and acceptor emission channels, respectively, and were set to a scaling factor of 1 for all measurements.

of FRET ratios provided by the biosensor under physiological conditions. Here, an AKAR biosensor^{6,42} with a reporter module consisting of mTurquoise and circularly permuted (cp)Venus FPs (AKAR4.1)³³ is used to monitor PKA activity in living cells. The response of the AKAR4.1 probe expressed in cells treated with a specific PKA agonist is used to characterize the performance of the system for measurements of changing FRET ratios.

Measurements of biosensor probe activity in the living animal. Once the imaging system has been validated using the FRET standards, and the performance of the biosensor has been verified in living cells in culture, the final step is to apply the information

collected in the *in vitro* studies to use the FRET probe to assay cellular function in a living animal. We use the expression of Ad AKAR4.1 in the mouse liver to demonstrate the use of this protocol to measure the activity of the PKA pathway *in vivo*.

Limitations of the approach

The protocol described here is designed for compatibility with the commonly available commercial TPLSM systems equipped with a single Ti-sapphire laser and detection pathways compatible with the emission spectra of CFP and YFP. We recognize that investigators may conduct their TPLSM studies on a shared instrument for which the non-descanned detectors may not be configured for the

efficient collection of cyan and yellow fluorescence. In this situation, it may be necessary to use the descanned detectors, which are typically easier to configure. As descanned detectors are located far from the back aperture of the objective, they collect less of the fluorescence scattered in the tissue, and thus provide poorer reach into biological tissues than non-descanned detectors located adjacent to the back aperture of the objective. The ideal design for a system dedicated to 2PE FRET studies would be one in which the non-descanned pathway were fitted with filters optimized for sensitive and specific detection of mTurquoise and mVenus.

In addition, the objective lenses used to obtain subcellular resolution provide a field of view that is typically less than a millimeter across. Therefore, it can be difficult to draw general conclusions about cellular function based on observations collected within such a tiny window. More importantly, the microscope samples only the most superficial layers of biological tissues. Even TPLSM, which allows deeper imaging than confocal microscopy, is generally limited to depths of < 100 μm into tissue. Thus, TPLSM is incapable of analyzing populations of cells located deep in organs (e.g., renal medulla) or evaluating physiological properties below the surface of tumors.

Finally, the intravital setting presents substantial challenges to the expression of fluorescent biosensor probes. Here, we use Ad transduction to achieve high-level expression of a biosensor probe in the liver of mice. The Ad provides robust, but transient, expression of the transgenes. Further, there are typically inflammatory responses to the virus that can limit its use in prolonged studies. These problems are largely overcome by adeno-associated virus (AAV) or lentivirus vectors, which can achieve persistent transgene expression with minimal inflammatory responses. Importantly, there are many serotypes of AAVs that differ in their capsid protein structures, and this enables distinct tissue tropism for the different serotypes^{20,43}.

Advantages

A crucial component of this protocol is the use of the well-characterized FRET standards as a tool to validate that both the

experimental model and the microscope system are optimized for sensitive measurements of FRET (ANTICIPATED RESULTS). Therefore, it is necessary that the end users determine the corrected FRET efficiency for each of the standards to assess the performance of their system and to compare their results with those obtained here (or from other studies, if different standards are used). The measurement of the FRET standards on the microscope system enables confirmation of the ratiometric FRET measurements acquired *in vivo* using the single-wavelength 2PE of the biosensor probes. The acquisition of single, two-channel images with TPLSM simplifies image collection, maximizing temporal resolution and minimizing the number of *in vivo* studies. The use of a single wavelength for 2PE offers additional advantages for the measurement of biosensor probe activity in intact tissue, avoiding delay in the collection of ratio images and the effects of shifts in laser alignment at different wavelengths.

Several groups have described the use of fluorescence lifetime imaging as an effective approach for measuring FRET *in vivo*^{44–46}. The ratiometric approach offers a few key advantages over fluorescence lifetime-based approaches. First, it is easily implemented in most TPLSM systems, requiring no additional instrumentation. Second, the ratiometric approach provides better temporal resolution; whereas fluorescence-lifetime measurements typically require image collection over tens of seconds, images for ratiometric measurements can be collected in less than a second.

We demonstrate the use of our approach to measure PKA activity *in vivo*. However, we emphasize that this approach should be generalizable to other FRET-based biosensors, once the reporter module is modified to include mTurquoise and a suitable acceptor. For example, we have found very similar results using the optimized calcium biosensor probe Twitch2b (ref. 47). Thus, with minimal effort, the approach described here can be applied to many other biosensor probes by exchanging the earlier, more photolabile, variants of the CFPs.

MATERIALS

REAGENTS

- DMEM (Thermo Fisher Scientific, cat. no. 50-188-267FP)
- DMEM without phenol red (Thermo Fisher Scientific, cat. no. MT17205CV)
- FBS (Atlanta Biologicals, cat. no. S11150)
- Opti-MEM I Reduced Serum Medium (Thermo Fisher Scientific, cat. no. 31985062)
- Trypsin, stored at $-20\text{ }^{\circ}\text{C}$ (Thermo Fisher Scientific, cat. no. MT25-051-Cl)
- X-tremeGene HP DNA Transfection Reagent (Roche Diagnostics, cat. no. 06366236001)
- Poly-D-lysine (Sigma-Aldrich, cat. no. P7280)
- FuGENE (Promega, cat. no. E2692)
- Lipofectamine 2000 (Thermo Fisher Scientific, cat. no. 11668019)
- Appropriate biosensor construct **▲ CRITICAL** In the procedure, we use the Ad CMV-Turq-AKAR4 vector as an example, which was made as described previously⁴⁸ (**Supplementary Data**).
- Human embryonic kidney (HEK)-293 cells (ATCC CRL-1573)
- **! CAUTION**—HEK-293 cells contain Ad 5 DNA integrated into chromosome 19 and must be handled at biosafety level 2. The cell lines used in your research should be regularly checked to ensure that they are authentic and that they are not infected with mycoplasma.
- FP constructs (see **Table 1**). All FP constructs described here are available through the National Institutes of Health O'Brien Center for Advanced Renal Microscopic Analysis at the Indiana University School of Medicine. The plasmid sequences can be found in the **Supplementary Data**

- Mice **! CAUTION** Any experiments involving live mice must conform to relevant institutional and national regulations. All animal studies were approved by the Indiana University School of Medicine Institutional Animal Care and Use Committee and conform to the 'Guide for the Care and Use of Laboratory Animals' published by the National Institutes of Health (NIH publication no. 85-23, revised 1996).

EQUIPMENT

- Laser-scanning microscope compatible with 2PE at 810 nm and two-channel fluorescence detection in the approximate ranges of 454–494 nm for detection of mTurquoise and 520–580 nm for detection of mVenus (our system is described in the Equipment Setup section)
- Image processing software capable of quantifying signal levels in user-identified regions of interest, such as ImageJ (<https://imagej.nih.gov/ij/>), Metamorph (<https://www.moleculardevices.com/>) or the microscope manufacturer's software
- A laser power meter to measure the power at the specimen plane (Thorlabs, model no. PM100D)
- Lab-Tek II four-well chambered coverglasses

REAGENT SETUP

HEK-293 cells Human embryonic kidney (HEK)-293 cells should be maintained in monolayer culture in DMEM containing 10% (vol/vol) FBS at 37 $^{\circ}\text{C}$ in a 5% (vol/vol) CO_2 incubator, and harvested at 80% confluence by treatment with trypsin. The pH indicator dye phenol red may cause background signals

TABLE 1 | FP constructs required in the procedure.

Plasmid construct	Purpose	Additional comments
mTurquoise N1	To determine donor spectral bleed-through	
mVenus N1	To determine acceptor spectral bleed-through	
Turquoise-TRAF-Venus (TTRAFV)	Serves as a low-FRET standard and is used to determine fractional excitation of Venus	Turquoise is separated from Venus by the TRAF2 sequence ⁴⁰ . A typical E_{FRET} value is 5–10%
Turquoise-10AA-Venus (T10V)	Serves as an intermediate FRET standard	Turquoise is separated from Venus by the sequence 'SGLRSPVAT'. A typical E_{FRET} value is 30–35%
Turquoise-5AA-Venus (T5V)	Serves as a high-FRET standard	Turquoise is separated from Venus by the sequence 'SGLRS'. A typical E_{FRET} value is 40–45%
Turquoise AKAR4.1	Biosensor probe to detect protein kinase A activity	The AKAR4 biosensor ⁴² with Turquoise as the donor fluorophore

during imaging. Therefore, before imaging, the medium should be replaced with the same medium lacking the indicator.

X-tremeGene HP DNA Transfection Reagent Make fresh solution according to the manufacturer's instructions before each experiment.

EQUIPMENT SETUP

Intravital microscope system In our laboratory, intravital microscopy (IVM) is conducted as previously described²⁴ using a modified Olympus FV1000 spectral laser-scanning confocal microscope system, mounted on an Olympus IX81 stand, and modified for 2PE. Near-IR illumination, provided

by a MaiTai HP Ti-sapphire laser (Spectra-Physics), is attenuated using a Pockels cell electro-optical attenuator (Conoptics), and the beam is expanded via a Keplerian collimator/beam expander. Images are acquired using an Olympus ×25, numerical aperture 1.05 XLPlan water-immersion objective (Fig. 1). Fluorescence is collected using the Olympus FV1000 photomultiplier detectors on the descanned detection pathway. A FV1000 spectral detection system (spectral grating) is used to collect spectral data and to select emission wavelengths optimized for each FP. Laser power at the specimen plane is measured using a PM100D power meter (Thorlabs).

PROCEDURE

Preparation of cells for imaging ● TIMING ~1 h plus overnight incubation

1 | *Transfection of cells with mTurquoise and mVenus plasmids.* 18–24 h before transfection, plate the HEK-293 cells in 500 μl of complete growth medium at a density of 3.0–3.5 × 10⁵ cells per well in Lab-Tek II four-well chambered coverglass. Incubate the cell cultures overnight in a 5% (vol/vol) CO₂ incubator. The cells should be 50–85% confluent at the time of transfection, and each transfection should be performed in duplicate.

2 | Allow X-tremeGENE HP DNA Transfection Reagent, DNA and diluent (Opti-MEM I Reduced Serum Medium or serum-free medium) to warm to room temperature (~21 °C), and gently mix.

3 | For each transfection, place 300 μl of diluent in a sterile tube.

4 | Add 3 μg of the appropriate plasmid DNA (see table below) to each transfection mix. Pipette gently to mix.

Transfected plasmid(s)	Step at which transfection is performed	Purpose
mTurquoise	4	Determining optimal settings for detection (Step 11) and spectral bleed-through (Step 13)
mVenus	4	Determining optimal settings for detection (Step 11) and spectral bleed-through (Step 13)
mTurquoise + mVenus	4	Determining fractional excitation at 810 nm (Step 16) and E_{FRET} value (Step 21)
Turquoise-TRAF-Venus (TTRAFV)	4	Determining fractional excitation at 810 nm (Step 16) and E_{FRET} value (Step 21)
Turquoise-5AA-Venus (T5V)	4	Determining E_{FRET} value (Step 21)
Turquoise-10AA-Venus (T10V)	4	Determining E_{FRET} value (Step 21)
AKAR4.1 biosensor (or probe of interest)	4	Biosensor probe for measurement of PKA activity (Step 27)



PROTOCOL

- 5| Add 9 μl of X-tremeGENE HP DNA Transfection Reagent to the diluted DNA (3:1 ratio of reagent to DNA). Pipette gently to mix.
- 6| Incubate the mixture for 15–30 min at room temperature.
- 7| Add 75 μl of the appropriate transfection complex to the cells in a drop-wise manner.
- 8| Gently shake the chambered coverglass to ensure even distribution, and then incubate the cells at 37 °C in 5% (vol/vol) CO_2 for 24–48 h before imaging.

System evaluation and optimization—determination of the spectral ranges for the detectors ● TIMING 1.5–2 h

9| *Prepare the TPLSM system.* At least 30 min before image acquisition, turn on the system according to the manufacturer instructions, to ensure that power and alignment are completely stabilized before image collection. Tune and align the laser at 810 nm.

▲ **CRITICAL STEP** Allow the laser to warm and stabilize for ~30 min before imaging to ensure that the system is consistent for image collection.

10| *Prepare to collect images for measurement of SBT.* 24–48 h after transfection of cells with mTurquoise or mVenus (at Step 4), transfer transfected cells (from Step 8) into a medium suitable for maintaining physiological pH in air, or into a chamber capable of maintaining a 5% (vol/vol) CO_2 environment. Mount the cells in a stage incubator set to maintain the cells at 37 °C.

11| Optimize the microscope settings for optimal detection of mTurquoise and mVenus emissions. Users with filter-based systems should follow option A to verify that the correct filters and mirrors are in use. Users with spectral fluorescence detectors should follow option B to determine the spectral-range settings for the imaging system.

▲ **CRITICAL STEP** The SBT components that contaminate the FRET signal result from the donor (mTurquoise) emission that bleeds into the acceptor detection channel (donor SBT (DSBT)), and the direct excitation of the acceptor (mVenus) at the donor excitation wavelength (acceptor SBT (ASBT)). It is necessary to correct for SBT in order to accurately determine FRET efficiency. The SBT corrections are specific to each microscope system, and they are entirely dependent on spectral or filter settings on the microscope; thus, it is critical to always verify these settings on multiuser microscope systems.

(A) Verification of the setup of filter-based systems

- (i) Select the correct emission filters for the cyan and yellow channels, and the appropriate dichroic mirror.
- (ii) Measure the signal from the cells expressing mTurquoise only and that from cells expressing mVenus only (from Step 8) to verify that the correct emission filters and dichroic mirrors are being used.

(B) Optimization of systems with spectral fluorescence detectors

- (i) Using cultured cells expressing mTurquoise only and cells expressing mVenus only (from Step 8), set the illumination to 810 nm, adjust illumination levels to fill the dynamic range of the detectors without saturation, and collect emission scans from ~420–600 nm.
- (ii) Evaluate the emission spectra of mTurquoise and mVenus, and identify the optimal wavelength ranges for selectively detecting mTurquoise and mVenus fluorescence emissions. For our system, these ranges were determined to be 454–494 for detection of mTurquoise and 520–580 for detection of mVenus (**Fig. 1**).

? TROUBLESHOOTING

System evaluation and optimization—SBT and fractional excitation ● TIMING 4 h

▲ **CRITICAL** This protocol uses a single excitation wavelength (810 nm) to measure FRET standard and biosensor activity. The FRET standards are used for system validation, so it is necessary to determine the corrected E_{FRET} for each standard excited at this wavelength (Step 21). This requires the measurement and removal of the DSBT and ASBT (Steps 13 and 16, and **Box 1**). As a single excitation wavelength is used, the determination of the ASBT also requires the estimation of the fractional excitation of Venus at 810 nm. This is accomplished by measuring the average $I_{\text{Ch2-810}}/I_{\text{Ch2-960}}$ ratio from cells expressing a mixture of mTurquoise and mVenus (mTurquoise + mVenus), as well as measuring the low-FRET standard (Turquoise-TRAF-Venus, Step 16).

12| *Collect images for measurement of SBT.* Designate 810 nm as the illumination wavelength, and select the optical configuration of the microscope system for optimal collection of CFP and YFP (determined in Step 11A for users with filter-based systems) or set optical configuration according to the results obtained in Step 11B (for users with spectral detection systems). Adjust the laser power to fill the dynamic range of the detectors without saturation. Collect two-channel images from living cells expressing mTurquoise only and from cells expressing mVenus only (from Step 8).

? TROUBLESHOOTING

13 | *Image analysis for measurement of SBT.* Using image-processing software (e.g., ImageJ, Metamorph or the microscope manufacturer's software), identify regions of interest in several cells (here and in subsequent steps, we typically aim for 5–10 cells) expressing mVenus only, and for each region measure the signal levels in the CFP and YFP channels. Correct these measurements for background by subtracting measurements obtained from nearby regions lacking fluorescence. For each cell, measure ASBT as the ratio of corrected measures obtained in the CFP channel to those obtained in the YFP channel. ASBT measurements are used to derive correction factor A (**Box 1**), which is defined as the fraction of the signal in the acceptor channel that results from the direct excitation of mVenus at 810 nm.

? TROUBLESHOOTING

14 | Using image-processing software, identify regions of interest in several cells expressing mTurquoise only. For each region, measure the signal levels in the CFP and YFP channels. The images are corrected for background by subtracting measurements obtained from nearby regions lacking fluorescence. For each cell, measure DSBT as the ratio of corrected measures obtained in the YFP channel to those obtained in the CFP channel. DSBT measures are used to derive correction factor B (**Box 1**), which is defined as the fraction of the signal in the acceptor channel that results from the bleed-through of the mTurquoise emission.

15 | *Collect images for measurement of fractional excitation of mVenus at 810 nm.* Using the same wavelengths, collect images of living cells expressing both mTurquoise and mVenus under conditions of minimal FRET (e.g., a mixture of the two, or a low-FRET standard, from Step 8), first with illumination at 810 nm and then again using illumination at 960 nm. Laser power at 960 nm should be adjusted to be equivalent to that used at 810 nm, as measured with a laser power meter at the specimen plane.

▲ **CRITICAL STEP** Tuning a Ti-sapphire laser to different wavelengths may lead to differences in laser alignment that can affect quantitative measures. It is critical to ensure that laser alignment is unaffected, or corrected, when changing between 810 and 960 nm.

? TROUBLESHOOTING

16 | *Image analysis for measuring fractional excitation of mVenus at 810 nm.* Using image-processing software (e.g., ImageJ, Metamorph or the microscope manufacturer's software), identify regions of interest in several cells expressing mVenus, and for each region measure the signal levels in the YFP channels when excited at 810 nm and when excited at 960 nm. Correct these measurements for background by subtracting measurements obtained from nearby regions lacking fluorescence. For each cell, measure the ratio of corrected signals obtained at 810-nm illumination to those measured at 960 nm. This ratio is used, along with ASBT, to derive correction factor A. The corrected FRET signal ($FRET_{corr}$) is determined by subtracting the cross-talk components A and B from the raw FRET signal (donor excitation, acceptor emission (**Box 1**)).

System validation—measurement of FRET in living cells expressing FRET-standard constructs ● **TIMING 6 h**

▲ **CRITICAL** The performance of the system is validated by measurement of FRET in cultured cells expressing the fully characterized FRET standard constructs. The determination of E_{FRET} for the known FRET standards enables users to assess the performance of their system and to compare their results with those obtained here (or from other studies, if different standards are used). To ensure that physiological measurements are not compromised by potential changes in the laser, optics or detectors, data should be collected for FRET standards with each physiological study.

17 | *Image collection for measurements of FRET standards.* 24–48 h before imaging, transfect the HEK293 cells (as described in Steps 1–8) with the FRET standard constructs—mTurquoise-TRAF-mVenus, mTurquoise-5AA-Venus, mTurquoise-10AA-Venus and a 1:1 mixture of mTurquoise and mVenus (Step 4).

? TROUBLESHOOTING

18 | Prepare the TPLSM system for imaging, as described in Step 9.

19 | Transfer transfected cells to a medium suitable for maintaining physiological pH in air, or to a chamber capable of maintaining a 5% (vol/vol) CO₂ environment. Mount the cells in a stage incubator set to maintain the cells at 37 °C.

20 | Using the same laser power and emission wavelength settings used in Steps 12 and 15, collect two-channel images of cells expressing each of the FRET standard constructs and cells coexpressing mTurquoise and mVenus (Step 4).

▲ **CRITICAL STEP** Transient co-transfection of cells with a mixture of the mTurquoise and mVenus plasmids will produce highly variable relative expression levels of the two different FPs. For this protocol, it is important to preselect cells for imaging that have intensity levels in both channels that are similar to the low-FRET efficiency standard (mTurquoise-TRAF-mVenus, which has a fixed 1:1 ratio of the donor and acceptor, with little donor quenching).

PROTOCOL

21 | *Image analysis for measurements of FRET standards.* Using image-processing software, identify regions of interest in several cells expressing FPs, and for each region measure the signal levels in the CFP and YFP channels. Correct these measurements for background by subtracting measurements obtained from nearby regions lacking fluorescence. For each cell, measure the FRET ratio and calculate E_{FRET} (**Box 1**).

▲ CRITICAL STEP The 2PE method described here should readily distinguish the three FRET standards with the different linker lengths from one another based on the measured E_{FRET} (see ANTICIPATED RESULTS). It is critical to use this approach to demonstrate that the TPLSM system is properly set up to obtain accurate measurements of E_{FRET} and is capable of high-sensitivity measurements from the biosensor probes in living cells.

? TROUBLESHOOTING

Validation of the FRET biosensor—measurement of the biosensor probe FRET response in cultured cells ● TIMING 5 h

▲ CRITICAL It is important to validate the performance of the biosensor in a cell model before studies in more complex systems. The response of the biosensor probe is evaluated in living cells following treatment with agents known to stimulate the relevant physiological response pathway. Here, the PKA agonist forskolin (Fsk) is used to test the response of the AKAR4.1 biosensor to PKA activation.

22 | *Image collection for measurements of FRET biosensor responses.* 24–48 h before imaging, transfect the HEK293 cells with the FRET biosensor (here, AKAR4.1), as described in Steps 1–8.

? TROUBLESHOOTING

23 | Prepare the TPLSM system for imaging, as described in Step 9.

24 | Transfer transfected cells to a medium suitable for maintaining physiological pH in air, or to a chamber capable of maintaining a 5% (vol/vol) CO₂ environment. Mount the cells in a stage incubator set to maintain the cells at 37 °C.

25 | Using the laser power and emission wavelength settings used in Steps 12, 15 and 17, collect a series of two-channel images of a field of cells expressing AKAR4.1 to establish baseline measurements.

26 | Collect a series of images before and after activating the biosensor probe. Here, images were collected at 30-s intervals before and after the addition of Fsk to the culture medium (final concentration of 24 μM). Fsk-mediated activation of PKA is expected to induce a rapid and significant increase in the Venus to Turquoise emission ratio (ANTICIPATED RESULTS).

? TROUBLESHOOTING

27 | *Image analysis for measurements of FRET biosensor responses.* Using image-processing software, identify regions of interest in several cells expressing AKAR4.1, and for each region measure the signal levels in the CFP and YFP channels. Correct these measurements for background by subtracting measurements obtained from nearby regions lacking fluorescence. For each cell at each time point, measure the normalized Venus to Turquoise emission ratio.

▲ CRITICAL STEP It is important to verify the function of the FRET-based biosensor probes using other methods, such as fluorescence-lifetime imaging microscopy or acceptor photobleaching measurements. In addition, it is important to demonstrate that the biosensor is reporting the correct cellular activity. Treatment of cells with unrelated signaling molecules or antagonists to the specific cellular pathway should not elicit the biosensor response. Moreover, point mutations in the bioactive linker (phosphorylation or binding sites) should abolish the changes in the probe response.

? TROUBLESHOOTING

Measurement of the biosensor probe FRET response in the organ of a living animal—intravital microscopy ● TIMING 9 h

▲ CRITICAL Once the biosensor has been validated, the 2PE ratiometric method can be used to measure biosensor probe activity in the targeted organ in a living animal. Here, we demonstrate the approach by measuring the effect of glucagon on PKA activity in cells in the intact mouse liver in mice transduced with the Ad AKAR4.1 vector.

28 | *Transduction of mice with a FRET biosensor.* 7 d before imaging, introduce 0.2 ml of the Ad AKAR4.1 vector (4.8×10^{10} particles) into mice by tail-vein injection, using standard methods (e.g., <http://www.procedureswithcare.org.uk/intravenous-injection-in-the-mouse/>).

! CAUTION All animal studies must be approved by the relevant institutional animal care and use committee and must conform to the applicable national regulations. Studies of animals transduced with Ad must be conducted in compliance with institutional biosafety standards.

29| *Image collection of FRET biosensor responses in the liver of a living mouse.* Physiological manipulations and animal preparations will vary according to the study. To prepare for activation of PKA in liver via glucagon⁴⁹, withdraw food from mice 3 h before scheduled imaging.

? TROUBLESHOOTING

30| Prepare the TPLSM system for imaging, as described in Step 9.

31| Externalize the left lateral lobe of the liver and prepare for IVM imaging through a glass-bottom plate using previously described methods²⁴.

32| Place the animal on the warmed microscope stage, identify a field of hepatocytes expressing AKAR4.1 and, using the same microscope settings used in Steps 12, 15, 17 and 26, collect a series of 3D image volumes (10 planes spanning 10 μm) in CFP and YFP channels to establish the baseline ratio. 3D stacks are collected to ensure sequential capture of hepatocyte cytosols despite residual vertical motion of the liver because of respiration.

33| Continue to collect 3D image volumes during and following IP injection of glucagon (200 μg/kg) to monitor the increase in the FRET ratio resulting from activation in PKA.

34| *Image analysis of FRET biosensor responses in the liver of a living mouse.* Using image-processing software, align and assemble image stacks into a sum of all planes for each channel and each time point.

35| Identify regions of interest in several cells expressing AKAR4.1 that display relatively uniform fluorescence. For each region, measure the signal levels in the CFP and YFP channels. Correct these measurements for background by subtracting measurements obtained from nearby regions lacking fluorescence. For each cell at each time point, measure the Venus to Turquoise emission ratio.

36| Pool and normalize the measured emission ratio data for all regions of interest.

? TROUBLESHOOTING

? TROUBLESHOOTING

Troubleshooting advice can be found in **Table 2**.

TABLE 2 | Troubleshooting table.

Step	Problem	Possible reason	Solution
11, 13	Substantial bleed-through of the acceptor signal in the donor channel is observed	The spectral bandwidth of the donor channel extends too far into the range of the acceptor emissions. The spectral bandwidth of the acceptor channel is too wide or an inappropriate dichroic mirror is used	Change the range of the spectral detector or change the band-pass filter for acceptor and/or donor emissions
	Substantial bleed-through of the donor signal into the acceptor channel	The spectral bandwidth of the donor channel extends too far into the range of the acceptor emissions or an inappropriate dichroic mirror is used	Change the range of the spectral detector or change the band-pass filter for acceptor and/or donor emissions
	Excessively high value of correction factor B	The spectral bandwidth of the donor channel extends too far into the range of the acceptor emissions or an inappropriate dichroic mirror is used	Change the range of the spectral detector or change the band-pass filter for acceptor and/or donor emissions
12, 15, 17, 22	Cells do not adhere to the coverslip properly, or they are not healthy	Coverslips are not coated with the appropriate matrix	Coat coverslips with poly-d-lysine or collagen
		Inappropriate culture conditions	Ensure that the culture conditions are optimized for the cell line used

(continued)

TABLE 2 | Troubleshooting table (continued).

Step	Problem	Possible reason	Solution
	Inadequate expression of fluorescent proteins in cultured cells	The transfection agent (FuGENE, Lipofectamine and X-tremeGene HP) or DNA plasmid concentration or their ratio is not optimized	Follow the transfection agent manufacturer's recommendations to vary the ratio of DNA: transfection agent or concentrations of DNA and/or transfection agent
12, 15, 17, 22, 29	Photobleaching is observed	The power of the excitation light is too high	Optimize the optical path and/or reduce laser power
	The signal fluctuates during TPLSM data acquisition	The laser illumination is unstable	Ensure that the laser is warmed for ~30 min before imaging. Ensure that the room temperature is stable
17, 22, 29	FRET measurements are obscured and/or altered by cell or tissue autofluorescence	Components in the specimen have fluorescence excitation properties at the donor 2PE wavelength	Avoid media with indicator dyes. Change the range of the spectral detector or change the band-pass filter for acceptor and/or donor emissions to minimize interference. Collect images from FRET standards expressed in the same cells or tissues used in studies of physiology
21	Spatial variation in ratios measured for the FRET standards	Chromatic aberration	Choose chromatically corrected optical components
		Variable illumination across the field	Ensure homogeneous illumination; restrict measurements to homogeneous regions
		Variable background across the field	Use local background subtraction for quantifications
		Spatial variation in photobleaching	Minimize illumination levels, and minimize the time spent identifying fields to collect
	FRET standards fail to produce the expected E_{FRET} values	Low levels of probe expression, resulting in high background contributions, errors in image processing or errors in SBT corrections	It is critical to verify the FRET measurements of the standards by multiple methods (e.g., sensitized emission, acceptor photobleaching, fluorescence lifetime) ³² . The different methods should provide the same E_{FRET} values for the standards
		Deterioration of TPLSM system performance	If comparison with previous studies indicates a decline in the imaging system performance, check the optical path for alignment issues, check all filter settings and measure laser power at the specimen plane to verify that it is the same as in previous studies. If this fails, call for microscope service
26, 27	Biosensor fails to respond as expected to physiological stimulation	Cells are not healthy	Ensure that the cells are healthy (Steps 1 and 2)
		Probe activator is ineffective	Ensure that the probe activator is fresh, appropriately handled and used at the correct concentration
		Deterioration of TPLSM system performance	If comparison with previous studies indicates a decline in the imaging system performance, check the optical path for alignment issues, check all filter settings and measure laser power at the specimen plane to verify that it is the same as in previous studies. If this fails, call for microscope service

(continued)

TABLE 2 | Troubleshooting table (continued).

Step	Problem	Possible reason	Solution
29, 36	Inadequate fluorescence signal levels in the animal	Inadequate expression of fluorescent proteins Excessive depth-dependent attenuation of fluorescence	Measure the viral titer Reduce the depth of image collection. Increase illumination level
	Fluorescence image decreases in intensity and/or clarity over time	Water has evaporated from the water-immersion objective	Replenish the water more frequently. Consider switching to oil, glycerol or silicon-oil immersion objectives

● TIMING

- Steps 1–8, cell transfection: ~1 h plus overnight incubation, ~24–48 h before imaging
- Steps 9 and 10, preparation of TPLSM system for imaging: ~0.5 h
- Step 11, determination of the spectral ranges of the detector channels: ~1 h
- Step 12, image collection for measurement of SBT: ~1 h
- Steps 13 and 14, image analysis for measurement of SBT: ~1 h
- Step 15, image collection for measurement of fractional excitation of mVenus at 810 nm: ~1 h
- Step 16, image analysis for measurement of fractional excitation of mVenus at 810 nm: ~1 h
- Steps 17–20, image collection for measurement of FRET standards in cultured cells: ~2 h
- Step 21, image analysis for measurement of FRET standards in cultured cells: ~4 h
- Steps 22–26, image collection for measurement of FRET biosensor responses in cultured cells: ~2 h
- Step 27, image analysis for measurement of FRET biosensor responses in cultured cells: ~3 h
- Step 28, transduction of mice with a FRET biosensor: ~1 h
- Steps 29–33, image collection for measurement of FRET biosensor responses in living mouse: ~4 h
- Steps 34–36, image analysis for measurement of FRET biosensor responses in living mouse: ~4 h
- Box 1, analysis of SBT for the determination of FRET efficiency: ~1 h

ANTICIPATED RESULTS

Measurements of the FRET standards using 2PE

The FRET standards are used to demonstrate that the experimental model and microscope system are optimized for sensitive measurements of E_{FRET} in living cells (Steps 17–21). If the SBT corrections are accurate (Box 1), then there should be very

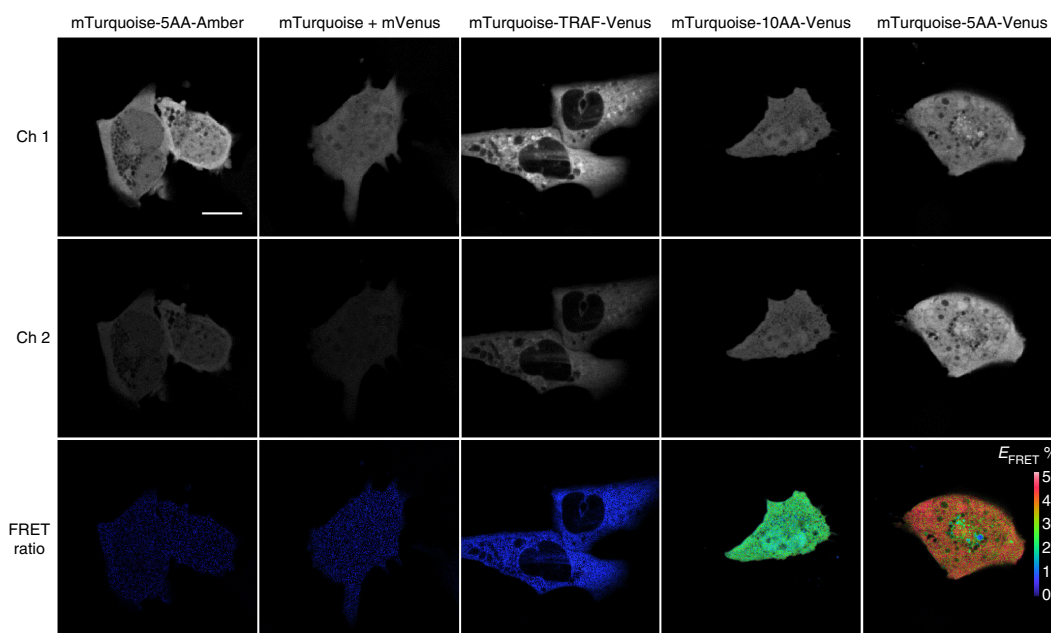


Figure 4 | FRET ratio images of HEK-293 cells expressing the indicated FRET standard probes. Cells were excited by illumination at 810 nm, and the mTurquoise (donor) intensity was measured in channel 1 (454–494 nm), whereas mVenus (acceptor) intensity was measured in channel 2 (520–580 nm). The FRET ratio images obtained from representative cells expressing the different FRET standard fusion proteins are shown. Scale bar, 10 μm. Image adapted with permission from ref. 33), American Physiological Society.

PROTOCOL

little energy transfer detected in cells that express a mixture of the unlinked mTurquoise and mVenus. The low-FRET-efficiency standard, mTurquoise-TRAF-mVenus, should also have a low, but measurable, E_{FRET} value (~5%)^{33,41,50}. By contrast, measurements from the cells expressing the highest E_{FRET} standard, mTurquoise-5AA-Venus, produce E_{FRET} values of ~45%. Critically, measurements from cells expressing the mTurquoise-10AA-Venus standard are expected to be ~36%, and should be readily distinguishable from the FRET standard with the shorter linker (**Fig. 4**). These FRET standards allow the validation of the imaging system, and provide a clear indication of the sensitivity of the measurements. The FRET standards also provide a control for identifying changes in performance of the laser, optics or detectors that may compromise measurements under physiological conditions.

2PE measurements of FRET-based biosensor probe activities in cultured cells

Biosensor validation is accomplished in studies in cultured cells expressing the biosensor that are treated with established methods to activate the cell-signaling event. For our studies, we transfected HEK293 cells with AKAR4.1 and monitored emissions in the cyan (454–494 nm) and yellow (520–580 nm) channels under illumination at 810 nm (Steps 22–27). After collecting a series of baseline images, the PKA agonist Fsk was added to a final concentration of 24 μM . As expected, Fsk induced a rapid and pronounced (1.4-fold) increase in the emission ratio of Ven/Turq (**Fig. 5**).

2PE measurements of FRET-based biosensor probe activities in living animals

After validation of the microscope system and the biosensor, studies are next conducted in living animals. For our studies, we took advantage of the robust tropism of Ad for the mouse liver following tail-vein injection²⁰ (Step 28). 7 d after injection with Ad AKAR4.1, the mice were fasted for 3 h, prepared for IVM, and then imaged as described above (Steps 29–33). Baseline images were collected, and imaging was continued after i.p. injection of glucagon (200 $\mu\text{g}/\text{kg}$), a treatment that has been previously shown to rapidly stimulate both cAMP and PKA in hepatocytes of fasted mice⁴⁹. Similar to the results obtained with HEK-293 cells treated with Fsk, glucagon treatment in the living mouse induced a rapid 1.4-fold change in the emission ratio of Ven/Turq (**Fig. 6**), indicating a rapid and sustained activation of PKA. A certain degree of cell–cell variability can be expected from cells *in vivo*; our earlier measurements³³ of 32 hepatocytes from three separate studies ranged from 1.14 to 1.827.

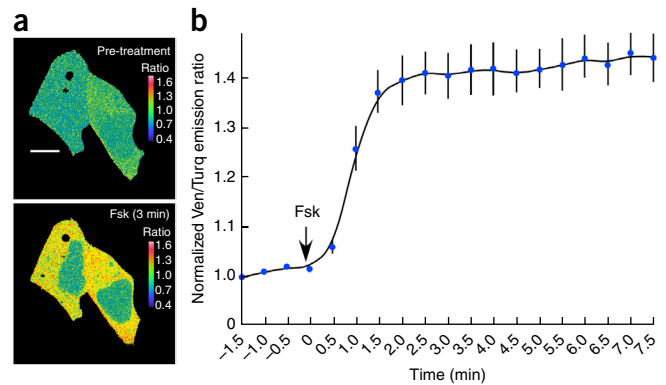


Figure 5 | Ratiometric FRET measurements from HEK-293 cells expressing the AKAR4.1 biosensor probe. (**a,b**) The cells were illuminated at 810 nm, and the emission signals were simultaneously measured in the mTurquoise (donor) channel (454–494 nm) and the mVenus (acceptor) channel (520–580 nm). The cells were treated with the protein kinase A (PKA) activator Forskolin (Fsk) to elicit changes in the FRET signal from the AKAR4.1 biosensor probe. (**a**) FRET ratio images of cells before (pretreatment) and 3 min after Fsk treatment. Scale bar, 10 μm . (**b**) The cells were treated with Fsk at time zero, and the acceptor to donor ratio (Ven/Turq) was measured every 30 s for 10 min. The Ven/Turq ratio was determined from 11 cells (\pm s.e.), as described in **Box 1**. Image adapted with permission from ref. 33), American Physiological Society.

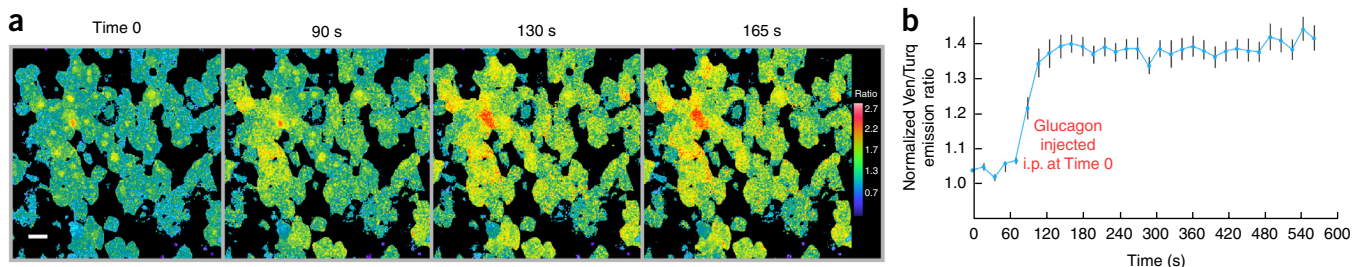


Figure 6 | Use of TPLSM to measure the response of the AKAR4.1 biosensor to glucagon in hepatocytes in the intact mouse liver. (**a,b**) The Ad AKAR4.1 viral particles were introduced by tail-vein injection and resulted in extensive expression in the liver 7 d later. (**a**) Ratio images from a single image plane in mouse liver at the indicated time points. Scale bar, 10 μm . (**b**) The mouse was treated by i.p. injection with glucagon (200 $\mu\text{g}/\text{kg}$) at time zero, and the acceptor to donor ratio (Ven/Turq) was measured every 15 s for 10 min. The Ven/Turq ratio was determined as described in **Box 1**, and the results are from the ten individual cells (\pm s.e. Image adapted with permission from ref. 33), American Physiological Society. All animal studies were approved by the Indiana University School of Medicine Institutional Animal Care and Use Committee and conform to the 'Guide for the Care and Use of Laboratory Animals' published by the National Institutes of Health (NIH publication no. 85-23, revised 1996).

Note: Any Supplementary Information and Source Data files are available in the online version of the paper.

ACKNOWLEDGMENTS This research was supported by the National Institutes of Health O'Brien Center for Advanced Renal Microscopic Analysis (NIH-NIDDK P30DK079312 to R.N.D. and K.W.D.). Microscopy studies were conducted at the Indiana Center for Biological Microscopy. The authors thank M. Kamocka and S. Winfree for their assistance in microscopy. This article is dedicated to the memory of M.W. Davidson.

AUTHOR CONTRIBUTIONS R.N.D. and K.W.D. wrote the manuscript. W.T. conducted the experiments, and R.N.D. and K.W.D. supervised the research.

COMPETING FINANCIAL INTERESTS The authors declare no competing financial interests.

Reprints and permissions information is available online at <http://www.nature.com/reprints/index.html>.

1. Day, R.N. & Davidson, M.W. *The Fluorescent Protein Revolution* (ed. Periasamy, A.) (Taylor & Francis, Boca Raton, FL, 2014).
2. Zhang, J., Campbell, R.E., Ting, A.Y. & Tsien, R.Y. Creating new fluorescent probes for cell biology. *Nat. Rev. Mol. Cell Biol.* **3**, 906–918 (2002).
3. VanEngelenburg, S.B. & Palmer, A.E. Fluorescent biosensors of protein function. *Curr. Opin. Chem. Biol.* **12**, 60–65 (2008).
4. DiPilato, L.M. & Zhang, J. Fluorescent protein-based biosensors: resolving spatiotemporal dynamics of signaling. *Curr. Opin. Chem. Biol.* **14**, 37–42 (2010).
5. Miyawaki, A. Development of probes for cellular functions using fluorescent proteins and fluorescence resonance energy transfer. *Annu. Rev. Biochem.* **80**, 357–373 (2011).
6. Zhang, J., Ma, Y., Taylor, S.S. & Tsien, R.Y. Genetically encoded reporters of protein kinase A activity reveal impact of substrate tethering. *Proc. Natl. Acad. Sci. USA* **98**, 14997–15002 (2001).
7. Patterson, G.H. & Piston, D.W. Photobleaching in two-photon excitation microscopy. *Biophys. J.* **78**, 2159–2162 (2000).
8. Chen, T.S., Zeng, S.Q., Luo, Q.M., Zhang, Z.H. & Zhou, W. High-order photobleaching of green fluorescent protein inside live cells in two-photon excitation microscopy. *Biochem. Biophys. Res. Commun.* **291**, 1272–1275 (2002).
9. Liu, L., Yermolaieva, O., Johnson, W.A., Abboud, F.M. & Welsh, M.J. Identification and function of thermosensory neurons in *Drosophila* larvae. *Nat. Neurosci.* **6**, 267–273 (2003).
10. Ben Arous, J., Tanizawa, Y., Rabinowitch, I., Chatenay, D. & Schafer, W.R. Automated imaging of neuronal activity in freely behaving *Caenorhabditis elegans*. *J. Neurosci. Methods* **187**, 229–234 (2010).
11. Kardash, E., Bandemer, J. & Raz, E. Imaging protein activity in live embryos using fluorescence resonance energy transfer biosensors. *Nat. Protoc.* **6**, 1835–1846 (2011).
12. Hara, M. *et al.* Imaging endoplasmic reticulum calcium with a fluorescent biosensor in transgenic mice. *Am. J. Physiol. Cell Physiol.* **287**, C932–C938 (2004).
13. Kamioka, Y. *et al.* Live imaging of protein kinase activities in transgenic mice expressing FRET biosensors. *Cell Struct. Funct.* **37**, 65–73 (2012).
14. Oldach, L. & Zhang, J. Genetically encoded fluorescent biosensors for live-cell visualization of protein phosphorylation. *Chem. Biol.* **21**, 186–197 (2014).
15. Aoki, K., Kamioka, Y. & Matsuda, M. Fluorescence resonance energy transfer imaging of cell signaling from *in vitro* to *in vivo*: basis of biosensor construction, live imaging, and image processing. *Dev. Growth Differ.* **55**, 515–522 (2013).
16. Berglund, K. *et al.* Imaging synaptic inhibition in transgenic mice expressing the chloride indicator, Clomeleon. *Brain Cell Biol.* **35**, 207–228 (2006).
17. Hausteiner, M.D. *et al.* Conditions and constraints for astrocyte calcium signaling in the hippocampal mossy fiber pathway. *Neuron* **82**, 413–429 (2014).
18. Madsen, L. *et al.* Transgenic mice for intersectional targeting of neural sensors and effectors with high specificity and performance. *Neuron* **85**, 942–958 (2015).
19. Johnsson, A.K. *et al.* The Rac-FRET mouse reveals tight spatiotemporal control of Rac activity in primary cells and tissues. *Cell Rep.* **6**, 1153–1164 (2014).
20. Buchholz, C.J., Friedel, T. & Buning, H. Surface-engineered viral vectors for selective and cell type-specific gene delivery. *Trends Biotechnol.* **33**, 777–790 (2015).

21. Babbey, C.M. *et al.* Quantitative intravital microscopy of hepatic transport. *Intravital* **1**, 44–53 (2012).
22. Dunn, K.W. *et al.* Functional studies of the kidney of living animals using multicolor two-photon microscopy. *Am. J. Physiol. Cell Physiol.* **283**, C905–C916 (2002).
23. Dunn, K.W., Sutton, T.A. & Sandoval, R.M. Live-animal imaging of renal function by multiphoton microscopy. *Curr. Protoc. Cytom.* **14**, 12.9 (2007).
24. Ryan, J.C., Dunn, K.W. & Decker, B.S. Effects of chronic kidney disease on liver transport: quantitative intravital microscopy of fluorescein transport in the rat liver. *Am. J. Physiol. Regul. Integr. Comp. Physiol.* **307**, R1488–R1492 (2014).
25. Presson, R.G. Jr. *et al.* Two-photon imaging within the murine thorax without respiratory and cardiac motion artifact. *Am. J. Pathol.* **179**, 75–82 (2011).
26. Vinegoni, C. *et al.* Sequential average segmented microscopy for high signal-to-noise ratio motion-artifact-free *in vivo* heart imaging. *Biomed. Opt. Express* **4**, 2095–2106 (2013).
27. Dombeck, D.A., Khabbazi, A.N., Collman, F., Adelman, T.L. & Tank, D.W. Imaging large-scale neural activity with cellular resolution in awake, mobile mice. *Neuron* **56**, 43–57 (2007).
28. Dunn, K.W., Lorenz, K.S., Salama, P. & Delp, E.J. IMART software for correction of motion artifacts in images collected in intravital microscopy. *Intravital* **3**, e28210 (2014).
29. Lee, S., Vinegoni, C., Sebas, M. & Weissleder, R. Automated motion artifact removal for intravital microscopy, without *a priori* information. *Sci. Rep.* **4**, 4507 (2014).
30. Lorenz, K.S., Salama, P., Dunn, K.W. & Delp, E.J. Digital correction of motion artefacts in microscopy image sequences collected from living animals using rigid and nonrigid registration. *J. Microsc.* **245**, 148–160 (2012).
31. Soulet, D., Pare, A., Coste, J. & Lacroix, S. Automated filtering of intrinsic movement artifacts during two-photon intravital microscopy. *PLoS One* **8**, e53942 (2013).
32. Radbruch, H. *et al.* Intravital FRET: probing cellular and tissue function. *Int. J. Mol. Sci.* **16**, 11713–11727 (2015).
33. Tao, W. *et al.* A practical method for monitoring FRET-based biosensors in living animals using two-photon microscopy. *Am. J. Physiol. Cell Physiol.* **309**, C724–C735 (2015).
34. Shaner, N.C. *et al.* Improving the photostability of bright monomeric orange and red fluorescent proteins. *Nat. Methods* **5**, 545–551 (2008).
35. Goedhart, J. *et al.* Bright cyan fluorescent protein variants identified by fluorescence lifetime screening. *Nat. Methods* **7**, 137–139 (2010).
36. Goedhart, J. *et al.* Structure-guided evolution of cyan fluorescent proteins towards a quantum yield of 93%. *Nat. Commun.* **3**, 751 (2012).
37. Markwardt, M.L. *et al.* An improved cerulean fluorescent protein with enhanced brightness and reduced reversible photoswitching. *PLoS One* **6**, e17896 (2011).
38. Zipfel, W.R., Williams, R.M. & Webb, W.W. Nonlinear magic: multiphoton microscopy in the biosciences. *Nat. Biotechnol.* **21**, 1369–1377 (2003).
39. Rizzo, M.A., Springer, G., Segawa, K., Zipfel, W.R. & Piston, D.W. Optimization of pairings and detection conditions for measurement of FRET between cyan and yellow fluorescent proteins. *Microsc. Microanal.* **12**, 238–254 (2006).
40. Nagai, T. *et al.* A variant of yellow fluorescent protein with fast and efficient maturation for cell-biological applications. *Nat. Biotechnol.* **20**, 87–90 (2002).
41. Thaler, C., Koushik, S.V., Blank, P.S. & Vogel, S.S. Quantitative multiphoton spectral imaging and its use for measuring resonance energy transfer. *Biophys. J.* **89**, 2736–2749.
42. Zhou, X., Herbst-Robinson, K.J. & Zhang, J. Visualizing dynamic activities of signaling enzymes using genetically encodable FRET-based biosensors from designs to applications. *Methods Enzymol.* **504**, 317–340 (2012).
43. Rincon, M.Y., VandenDriessche, T. & Chuah, M.K. Gene therapy for cardiovascular disease: advances in vector development, targeting, and delivery for clinical translation. *Cardiovasc. Res.* **108**, 4–20 (2015).
44. McGhee, E.J. *et al.* FLIM-FRET imaging *in vivo* reveals 3D-environment spatially regulates RhoGTPase activity during cancer cell invasion. *Small GTPases* **2**, 239–244 (2011).
45. Nobis, M. *et al.* Intravital FLIM-FRET imaging reveals dasatinib-induced spatial control of src in pancreatic cancer. *Cancer Res.* **73**, 4674–4686 (2013).



PROTOCOL

46. Janssen, A., Beerling, E., Medema, R. & van Rheenen, J. Intravital FRET imaging of tumor cell viability and mitosis during chemotherapy. *PLoS One* **8**, e64029 (2013).
47. Thestrup, T. *et al.* Optimized ratiometric calcium sensors for functional *in vivo* imaging of neurons and T lymphocytes. *Nat. Methods* **11**, 175–182 (2014).
48. Luo, J. *et al.* A protocol for rapid generation of recombinant adenoviruses using the AdEasy system. *Nat. Protoc.* **2**, 1236–1247 (2007).
49. Miller, R.A. *et al.* Biguanides suppress hepatic glucagon signaling by decreasing production of cyclic AMP. *Nature* **494**, 256–260 (2013).
50. Day, R.N. Measuring protein interactions using Forster resonance energy transfer and fluorescence lifetime imaging microscopy. *Methods* **66**, 200–207 (2014).
51. Broussard, J.A., Rappaz, B., Webb, D.J. & Brown, C.M. Fluorescence resonance energy transfer microscopy as demonstrated by measuring the activation of the serine/threonine kinase Akt. *Nat. Protoc.* **8**, 265–281 (2013).
52. Periasamy, A. & Day, R.N. *Molecular Imaging: FRET Microscopy and Spectroscopy* (Oxford University Press, New York, 2005).